Hypothesis

HLA-B27 lacking associated β2-microglobulin rearranges to auto-display or cross-display residues 169–181: a novel molecular mechanism for spondyloarthropathies

Manni Luthra-Guptasarma[a,*], Balvinder Singh[b]

[a]*Department of Immunopathology, Postgraduate Institute of Medical Education and Research (PGIMER), Chandigarh 160 012, India*
[b]*Institute of Microbial Technology (IMTECH), Chandigarh 160 036, India*

Received 21 June 2004; revised 9 August 2004; accepted 18 August 2004

Available online 28 August 2004

Edited by Michael R. Bubb

Abstract Expression of the MHC class I allelle, HLA-B27, is correlated with autoimmune disease. The misfolding and association of B27 heavy chains through non-native disulfide bonds has recently been implicated. Here, we propose that β2m-free, peptide-free heavy chains support a helix-coil transition in the segment leading from the α2 domain to the α3 domain, facilitating rotation of backbone angles around residues 167/168, and allowing residues 169–181 (identical to a known B27 ligand) to loop around and occupy the molecule's own peptide-binding cleft. Such 'auto-display', occurring either within B27 molecules, or between B27 molecules, could provoke autoimmune attack.

Keywords: HLA-B27; Ankylosing spondylitis; Protein misfolding; Detailed molecular mechanism; MHC auto display; Autoimmune disorders

1. Introduction

The autoimmune disease, ankylosing spondylytis (AS), is known to have a greater than 90% correspondence with the expression of HLA-B27, a Class I MHC protein [1]. The molecular mechanisms responsible for this correspondence are not yet understood. Previous hypotheses have focused on several possibilities, which are summarized below:

(A) *Antigenic (arthritogenic) peptide display by B27*. Investigators have explored the possible presentation of bacterial antigens, or bacterial antigen-like self peptides (including B27-derived peptides) by either B27 itself, or by other MHC Class I chains, or MHC Class II chains [2–8]. However, no mechanism explaining this disease has emerged.

(B) *Structural organization of β2-microglobulin (β2m)-free B27*. Unlike other MHC Class I chains that only become competent for peptide-binding in their β2m-bound forms, B27 chains in the β2m-free form have been observed to (i) bind peptides [9] and (ii) display a tendency to associate into large aggregates as well as homodimers stabilized structurally by disulfide-bonds formed between chains [10,11]. Since the rates and efficiencies of association of β2m with different MHC Class I chains vary widely [12], and it is also known that β2m tends to be shed by cell surface MHC complexes [13], it is considered possible that B27 chains lacking bound β2m appear on the cell surface in a peptide-displaying, structure-retaining form that may be somehow linked to disease; however, the actual experimental evidence currently available to show that β2m-free B27 binds peptides [9] still needs to be treated with some caution, at least until there is a larger body of evidence to support it. Some models involving disulfide bonding of Cys67 have been advanced [11], whereas a recent proposal also suggests the involvement of both Cys67 and Cys164 [14], in addition to a link between homodimer formation and the kinetics of assembly of HLA chains with the β2m subunit. Despite the obvious novelty and elegance of some of these proposals, the exact nature of the β2m-free form (or forms) that might stimulate autoimmunity still remains to be established, leaving open scope for further discussions and hypotheses.

(C) *Amyloid formation by surface-shed β2m*. The possibility has been raised that release of β2m chains by cell-surface B27 results in the deposition of β2m in synovial fluids in the form of amyloid aggregates, inviting immune responses against such aggregates [15]. In this particular scheme, of course, B27 itself remains incidental (rather than central) to the disease mechanism.

(D) *Production of anti-B27 antibodies*. Antibodies against B27 chains that also show some cross-reactivity with other MHC Class I chains have been detected in diseased patients [6,16]. Because B27 is a 'self' protein, immunological dogma would normally suggest that in the absence of associated defects in immune system development and/or functioning, no antibodies to such a protein should be produced. Thus, the presence of antibodies indicates possible additional involvement of the T-cell-independent B-cell arm of the immune system in the etiology of disease. The exact mechanisms, if any, remain to be deciphered.

In this paper, a novel molecular rationalization is proposed which reconciles three out of the four possibilities (A, B and D) above into a single mechanistic explanation for how a particular misfolded form of B27 could invite autoimmune attack.

* Corresponding author. Fax: +91-172-2744401.
E-mail address: mlg@glide.net.in (M. Luthra-Guptasarma).

0014-5793/$22.00
doi:10.1016/j.febslet.2004.08.037

2. The hypothesis

2.1. Conformational and associational equilibria of β2m-free and β2m-bound forms

Fig. 1(a) shows a regular ribbon-diagram representation of the B27 chain in its β2m-bound, peptide-bound form. In the previous section, we have already reviewed evidence that β2m-free B27 is capable of binding to, and displaying, peptides. Therefore, a schematic representing such a peptide-bound, but β2m-free form of B27 is shown in Fig. 1(b), essentially to emphasize that this form could be in dynamic equilibrium with the form shown in Fig. 1(a). Notably, in this form, whereas the structure of the first two domains of B27 (α1 and α2) is thought to be native-like, the third domain (α3) may be conceived to be swinging around in the solvent because there is no β2m present to bind and stabilize the domain in relation to the main part of the molecule that operates to bind to the peptide ligand. A third form that could potentially be in equilibrium with these two forms would be a peptide-free, as well as β2m-free, form of B27 as shown in Fig. 1(c). The implicit assumption for this form to exist detectably, of course, would be that β2m-free B27 would have a sufficiently lowered affinity for peptide to allow peptides to dissociate and reassociate with the pocket of the β2m-free B27. A fourth conceivable population participating in the equilibrium is a β2m-free form that is also not bound by a peptide ligand but which is conformationally altered, however, in a manner that allows a section of its own chain (identical in sequence to a known B27 ligand) to occupy its peptide-binding cleft through an act of autodisplay (as discussed later) facilitated by the absence of β2m. This fourth form is represented in Fig. 1(d).

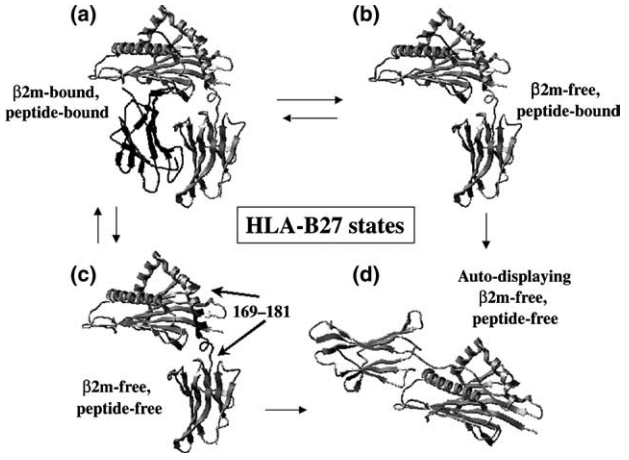

Fig. 1. Proposed equilibria amongst various associational and conformational states of HLA-B27. Details are marked on the figures, and described in the main text. In panels a and b, the schematic purports to show the peptide, N-RRYLENGKETLQR-C, bound to the peptide-binding cleft (in actual fact, the figure is based on coordinates for another bound peptide, N-GRFAAAIAK-C). In panel b, the bound peptide is still shown; however, without the associated β2m subunit. In panel c, the cleft is empty; however, the region of the B27 chain containing the sequence RRYLENGKETLQR (comprising residues 169–181, identical to a known B27 ligand peptide) is shown in dark black. This region consists partly of a helix and partly of an interdomain chain segment of irregular structure that leads from domains α1/α2 (the peptide-binding section) into domain α3. In panel d, this region is shown to have undergone a helix-coil transition, and looped around to bind to the peptide-binding cleft lying next to it (accompanied by movement of α3 with respect to α 1/α2) in the same binding configuration adopted by the separately bound peptide shown in panels a and b.

The view of the peptide-binding section of the B27 molecule (comprising its α1 and α2 domains) presented in Fig. 1(a)–(d) is the same; however, since in Fig. 1(d) the geometric relationship of the α3 domain with the α1 and α2 domains is changed to allow residues 169–181 to bind, this fact is only noted upon careful observation. Further, it must be remarked that these figures do not attempt to depict possible interactions amongst β2m-free B27 chains occurring, e.g., through one chain binding a polypeptide segment of a neighboring chain, as the complexity of such interactions lies outside the pale of what may be shown simply with a schematic diagram. We also wish to draw attention to the fact that none of the figures in this paper show the cell membrane; however, it may be assumed that in all cases where the α3 domain is shown, its C-terminal section is implicitly assumed to be linked to the roughly 25 residues-long hydrophobic tail of the B27 molecule that anchors the B27 heavy chain to the membrane.

2.2. The scope for self-display

A sequence of amino acids within the B27 chain (RRYLENGKETLQR) spanning residues 169–181 is homologous to certain bacterial proteins believed to be arthritogenic. From amongst the residues in this region of the B27 chain, the stretch comprising residues 168–176 has been shown to bind to the peptide-binding groove of B27 when it is presented to β2m-bound B27 as a free peptide [2]; a somewhat longer stretch of residues, comprising residues 169–179, has been shown to be a natural ligand of the B2705 and B2702 disease-associated subtypes of B27, but not of the B2703 subtype that shows poor association with disease [7,8,17]; an even longer stretch of residues from this region, comprising residues 169–181, has been shown to be a natural ligand of the B2705 subtype. Initially, these discoveries gave rise to the view that peptides containing residue sequences from this region are generated through proteolytic processing of B27, leading to their binding and display to the immune system. However, no clear rationalization of exactly why this leads to disease has ever emerged. Below, we offer a viable alternative.

2.3. A structural mechanism for auto-(self)-display

Structurally, residue 169 falls just after a junction separating two contiguous, almost co-directional helices differing very slightly in orientation (see Fig. 1(c)). The first of these helices forms a wall of the B27 peptide-binding cleft. As the figure shows, the junction of the two helices lies extremely close to the N-terminus of the peptide occupying the cleft of B27. Now, we may note that this peptide lying within the cleft of the B27 molecule could very well have been the peptide, N-RRYLENGKETLQR-C, that is known to be identical in sequence to residues 169–181 of the B27 chain itself. Of course, it must be mentioned that in the crystal structure coordinate file that was used to create the schematic shown in Fig. 1(c), the sequence of the peptide bound to B27 was actually N-GRFAAAIAK-C; however, this is an insignificant detail since, in any case, the figure is merely a schematic meant to convey the idea that the location of the N-terminus of the normally bound peptide is very close to residues 167 and 168 which precede a chain segment capable of binding to the B27 cleft. Residue 169 is located just after the junction, at the beginning of the second helix leading out of the cleft and directly into a

chain segment of irregular secondary structure that serves to join the first two domains of the B27 chain, α1 and α2, to the third domain, α3. It would be obvious from Fig. 1(a) that the geometric relationship of α3 to the α1 and α2 domains (comprising the peptide-binding section of the molecule) is determined principally by the binding of β2m, since this subunit binds both to α3 and to the beta sheet floor of the peptide-binding section formed by domains α1 and α2. Thus, in the absence of β2m there are unlikely to be enough stabilizing contacts to keep the interdomain chain segment structured. As a consequence, the α3 domain is likely to become mobile with respect to the peptide-binding section. Therefore, in the β2m-free form, (i) the loss of structure in the interdomain chain segment and (ii) the consequent mobility of the α3 domain could cause destabilization of the immediately preceding helix containing residues 169–181 since this helix, in any case, makes very few contacts with other regions of the chain. In the absence of bound-β2m, therefore, we propose that this helix simply unravels to adopt a randomly coiled conformation. Since it contains a part of the amino acid sequence cognate to the pocket (N-RRYLENGKETLQR-C, comprising residues 169–181) and is also proximal to the cleft, we further propose that motions of the α3 domain with respect to the peptide-binding section allow the chain to simply form a short loop allowing residues 169–181 to bind to the peptide-binding cleft. Of course, this is accompanied by a change in the geometric relationships amongst the domains, as suggested by the schematic shown in Fig. 1(d); however, the structures of the individual domains are conceived to remain largely native-like, with the exception of the regions around the peptide-binding cleft.

Since the α3 domain is anchored to the membrane through a long hydrophobic tail of about 25 residues, the increased flexibility (in the absence of β2m) within the interdomain segment separating the α3 domain from the peptide-binding section could be conceived to facilitate the following detailed changes in the geometric relationship amongst domains. Ordinarily, the short inter-domain segment emerges from the helix situated at one end of the peptide-binding cleft (i.e., the end that is proximal to the N-terminus of any bound peptide). The segment then descends to connect to the α3 domain stabilized by interactions with β2m. In the absence of β2m, upon the occurrence of the helix-coil transition, the interdomain segment of about 5–6 residues becomes essentially made longer by an additional 7 residues that are added onto its N-terminal end through the unfolding of the helix beginning at residue 169 (2 turns; 3.4 residues per turn). Therefore, nearly 12–13 residues are now available in the form of a random coil. As is well known, the polypeptide backbones of random coils contain two bonds per residue around which rotation can occur with ease, since only the peptide bonds in the backbone are rotationally restrained. This rotational freedom of the random coil allows it to flex itself in various ways with respect to flanking domain structures. We propose that the lengthening of the interdomain segment as a result of helix unfolding allows the segment to now explore and occupy the peptide-binding cleft so that it can traverse the entire length of the cleft (about 9 residues) before descending to meet the α3 domain, from the opposite end of the cleft. Of course, with respect to the membrane-anchored α3 domain, this would probably end up involving an effective rotation of the peptide-binding section (including the floor of the peptide-binding cleft) by about 180 degrees, around an axis roughly perpendicular to the membrane. Following this transformation, the peptide-binding cleft would still face away from the membrane with its floor positioned roughly parallel to the membrane. At any rate, even if this were not exactly so, it might be envisaged that the auto-displaying cleft would still remain accessible to T-cell receptors, since the only transformation occurring would be that the interdomain segment would traverse the cleft and descend to meet the α3 domain from the opposite end of the cleft from the one from which it ordinarily descends; sufficient flexibility could be expected to remain in the interdomain segment (residues 180–186), and also in the region between the α3 domain and the membrane spanning domain, to allow TCRs to access the altered peptide-binding segment.

Classically, MHC Class I chains are known to largely bind nonameric peptides [18,19]. Here, however, given the conformational changes proposed, it may be envisaged that the restrictions ordinarily applicable to the ends of the peptide-binding cleft remain no longer applicable due to the changes occurring at the ends of the cleft. In the next section of this paper, we present molecular modeling studies that appear to support the feasibility of the structural changes envisaged above.

3. Support from molecular modeling studies

The coordinates for the complex of HLA-B27 with a nonameric peptide ligand, N-GRFAAAIAK-C, were obtained from the RCSB database (file name: 1K5N.pdb). Using Insight II (2000) software, CVFF force fields, and a Silicon Graphics Fuel workstation for modeling, the chains corresponding to the (a) nonameric peptide ligand and (b) B27-associated β2m subunit were deliberately removed from the structure coordinate file, to leave only the atoms and coordinates corresponding to the heavy chain of B27. The backbone dihedral angles for residues 167 and 168 of the B27 chain were then rotated to allow residues 169–181 to be roughly juxtaposed opposite to the (now empty) peptide-binding cleft of B27; however, this was done without changing any other structural parameter or altering the short helical region of the chain following residue 167 and preceding the linker region leading into the α3 domain. The structures of two stretches of the chain comprising residues 1–167, and 182–276, were kept restrained, so that any structural freedom would be available to only the stretch between residues 168 and 181. The structure generated through the changes in dihedral angles was then minimized through a combination of steepest descent and conjugate gradient methods, using a convergence criterion of 0.1, to obtain a suitable starting conformation for residues 169–181 for use in molecular dynamics simulations. High temperature dynamics was performed, using the same conformational restraints as before, with 50 cycles of heating to 500 K (at the rate of 50 K per ps) and cooling to 300 K (at the rate of 30 K per ps), followed by 30 ps of molecular dynamics simulations at 300 K. Structure minimization for the best 50 structures was then carried out, this time without structural restraints, with a convergence criterion of 0.01. All MD calculations were performed with a distance-dependent dielectric, i.e., with implicit solvent rather than with explicit solvent involving water molecules.

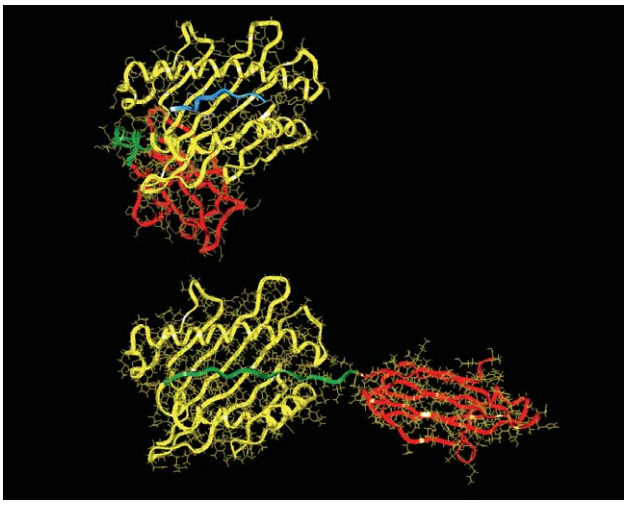

Fig. 2. The structure at the top is the structure of the B27 chain, shown bound to a peptide, N-GRFAAAIAK-C. The peptide is shown in blue. The combined α1 and α2 domains of the B27 chain are shown in yellow, while the α3 domain of the same chain is shown in red (behind α1 and α2). The region of the chain comprising a helix and an unstructured linker leading into α3 is shown in green. The β2m subunit implicit to this structure is not shown, to simplify the visual representation and to facilitate direct comparison with the remodeled structure shown in the lower panel. The lower panel shows the modeled structure. This was obtained (a) by changing backbone dihedral angles of residues 167 and 168 [to turn the green section of the chain around to juxtapose residues 169–181 opposite to the peptide-binding cleft and change the geometric relationship of the α1/α2 (yellow) and α3 (red) domains], and (b) by carrying out a combination of structure minimization and molecular dynamic simulations. The region shown in green (including a helical section, and a region of the chain in irregular structure) is seen to have transformed into extended conformation, thus allowing this section of the chain to bind to the molecule's own peptide-binding cleft, in the absence of peptide (blue).

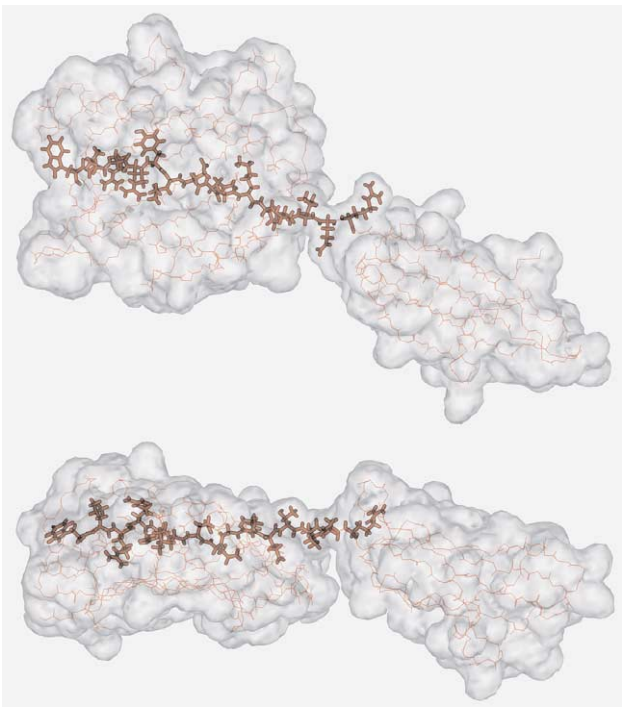

Fig. 3. Detailed structure of the B27 chain engaged in auto-display, derived through molecular dynamics performed for the equivalent of over 3000 ps of simulations. The upper panel shows the view of the molecule as one looks down upon the peptide-binding cleft from above. The lower panel shows the side-view, obtained by turning the view shown in the upper panel by 90° around a horizontal axis. The polypeptide is shown superimposed upon a transparent rendition of the molecule's surface. The use of transparency along with orthogonal views facilitates simultaneous assessment of the depth and intimacy of interactions occurring within the cleft. In both panels, the large mass on the left represents the combined α1 and α2 domains, while the smaller mass on the right shows the α3 domain which is anchored through a C-terminal hydrophobic domain (not shown) to the membrane. The section of residues from W166 to R181 is shown entering and occupying the peptide-binding cleft in an all-atom (thick bonds) CPK representation. The remaining molecule is shown in a backbone-only (thin bonds) CPK representation. R170 occupies pocket D, Y171 occupies pocket B, K176 occupies pocket C, and E 177 occupies pocket F.

The results of this study are presented in the form of a structure shown in the bottom panel of Fig. 2, which represents a real minimized structure that also serves simultaneously as a good schematic representation of the proposed changes in the molecule, with color coding of different sections (as described in the figure legend). It may be noted from inspection of this structure that the second helix in the wall of the peptide-binding cleft (which was proposed to undergo a helix-coil transition) is no longer a helix. Rather, the helix would appear to have rearranged, following high temperature dynamics, to cause the entire region of the chain to adopt an extended conformation that (following further molecular dynamics and minimization) happens to optimally position residues 169–181 into the peptide-binding cleft, by forming a loop at the point in the chain (near 167 and 168) earlier placed at the beginning of a short helix leading into the α3 domain. It may also be noted that some crucial residues ordinarily contributing to the formation of pocket A in the peptide-binding cleft (e.g., W167 and Y171) are relocated such that pocket A no longer exists. These residues are now engaged in supporting the extended conformation of the residues entering and occupying the cleft. The fact that this structure survived MD simulations over 30 ps suggests that it is a reasonably stable structure, as well as a feasible structure. For comparison, the normal structure of the B27 chain in complex with bound peptide (however, not showing the β2m) is shown as the top panel of Fig. 2. Comparison of the clefts in the two structures reveals structural readjustments in the auto-displaying chain.

We wished to further explore the kinetic stability of this structure through longer MD simulations, and carry out a more detailed examination of what would appear to be happening inside the cleft. Therefore, a further 3000 ps of simulations was performed at 300 K. Initially, this was attempted with explicit solvent included (i.e., with water molecules inside a box enclosing all protein atoms), with no conformational restraints. However, such simulations proceeded extremely slowly given the available system resources, with dynamics proceeding at the rate of only a few picoseconds per week. Therefore, after only about 10 ps of such simulations, we switched to an implicit solvent mode (with distance-dependent dielectrics), and with restraints imposed on all residues other than the stretch within the pocket, to complete several thousand picoseconds of simulations and examine whether the stretch was still within the cleft. The minimized structure derived from this study is shown in Fig. 3 in the form of two

views: the top view shows the cleft from above, while the bottom view shows the cleft from the side. The peptide positioned within the groove is depicted through a CPK representation that uses thick bonds, showing all atoms embedded within a surface representation that has deliberately been kept 'transparent' to allow simultaneous viewing of both the molecule's overall surface and the topology of its chain. For this purpose, the rest of the B27 molecule is also shown through a CPK representation; however, this is done through the depiction of only backbone atoms, again embedded within a transparent surface representation of all atoms, this time with thin bonds used to show the backbone. The two views are being deliberately shown to allow viewers to see the molecular surface while at the same time: (a) distinguishing between the sections of the B27 molecule forming the cleft and the section bound within the cleft and (b) ascertaining that the peptide is well ensconced and buried deep within the cleft. The surface representation indicates an optimized and intimate set of interactions of the cleft with its contents, in the minimized structure.

Detailed analysis of the conformation of the bound peptide within the cleft, through calculation of atom–atom distances between residues forming the cleft and those occupying the cleft suggests the following. At one end of the cleft, pocket A no longer exists, as already mentioned. Ordinarily, residue 62 locks in the N-terminus of any peptide bound in the cleft. However, with the rearrangement of other residues constituting pocket A, such as residues 167 and 171, the lock on this end of the cleft is effectively removed, allowing the polypeptide chain to enter the cleft. At the other end of the cleft, where the chain emerges to meet the α3 domain, residue K176 appears to occupy pocket C, whereas residue E177 appears to occupy pocket F. This is in consonance with the ninth residue from residue R169 entering pocket F, as would be expected. Perhaps, owing to the absence of pocket A whose occupation by the first residue of a nonameric peptide sets the tone for the entry of the remaining residues into the various pockets, rotations in the backbone appear to have caused residue R170 to enter pocket D instead of the expected occupancy of pocket B by this residue. Residue Y171, which would have been expected to enter pocket D, instead enters pocket B, and does so in such an intimate manner that the ring of the tyrosine sidechain cannot even be seen in an all-atom top-view if the surface is not made deliberately transparent as done for the top panel of Fig. 3. Thus, some non-canonical interactions are observed as may be expected, even though the sequence of residues anticipated to enter the cleft can be seen to have entered and occupied the cleft in an intimate and apparently optimized manner. It may be noted for the record that identification of the various pockets in the remodeled B27 chain was carried out through analysis of residue configurations that ordinarily define pockets in B27 chains as could be gleaned from the existing literature, in which lists of residues in a nonamer sequence that ordinarily enter the various pockets are available [18], as are lists of residues making up the various pockets themselves [20].

4. Correlate: appearance of β2m-free B27 with disease

There is evidence that the availability of free β2m in serum increases with autoimmune disease [21,22]. Whether this is a cause, or a consequence, of disease is not clear. It remains conceivable, however, that the increase in free β2m levels signals an increase in the availability of β2m-free HLA chains on the cell surface. If the cause behind shedding of β2m is something that happens in adult life due to some yet unknown stimulus, it is possible that auto-displaying B27 only comes into existence in the later years during development of disease and that, therefore, this form does not exist in the embryo, or in very young persons expressing the allele. Therefore, it may be assumed that the immune system does not ordinarily see this form, or naturally effect clonal deletion of cells during the period in which discrimination of self from non-self is effected. Therefore, it is possible that during the critical period of thymic education, β2m-free B27 chains are not presented to the immune system, such that T-cells bearing receptors cognate to such chains do not get eliminated in the thymus.

5. Auto-displaying B27 should appear 'foreign' to T-cells and B-cells

What are the immunological consequences of B27 ''auto-display''? For one thing, it may be held that the structural alterations involved in auto-display could create new conformational epitopes that would appear 'foreign' enough to the circulating population of naïve B-cells, allowing binding of some B-cells bearing cognate immunoglobulin receptors to cells presenting auto-displaying B27. Simultaneously, the structural alterations occurring in-and-around the binding cleft could lead to the occupied cleft also appearing sufficiently 'foreign' in structural format to the T-cell population, allowing binding of some T-cells through their T-cell receptors. Therefore, helper T-cells could cause activation of the naïve B-cells binding to autodisplaying B27, and themselves become activated in the process. Independently, it has also been recently reported that B27 is capable of interacting non-canonically with the CD4 receptor [23], bringing into question one of the most deeply entrenched dogmas concerning MHC Class I interactions with other immune system components. Binding of T-cells to autodisplaying B27 in this manner could lead to direct attack by effector T-cells. A further interesting possibility is that naïve B-cells could even be activated through T-independent mechanisms. As is well known, sugars such as lipopolysaccharides (LPS) that display many copies of a given carbohydrate-based B-cell epitope over the length of a long polymeric sugar structure manage to activate B-cells without any T-cell involvement, due to the ability of such sugars to effect a cross-linking of B-cell receptors. In this context, it has recently been suggested [24] that protein aggregates (especially if formed amongst proteins displayed on a cell surface) can also similarly activate B-cells through a T-independent mechanism, since protein aggregates would be likely to display multiple copies of a misfolding-derived conformationally foreign epitope to naïve B-cells over the length and breadth of a pseudo-polymer-like substratum provided by the aggregation process itself, to effect cross-linking of B-cell receptors on the surface of a naïve B-cell. Since, as we have already discussed, B27 heavy chains can conceivably form large assemblies of conformationally foreign chains through cross-display occurring amongst neighboring molecules, such assemblies might elicit activation of B-cells and eventually lead to the produc-

tion of antibodies. Such varied mechanisms, or a combination thereof, might potentially help rationalize both the presence of antibodies in AS patients and the T-cell mediated immune attack that is characteristic of such auto-immune disease.

6. Discussion and conclusions

We have proposed a detailed mechanism for the misfolding of the HLA-B27 heavy chain in the absence of β2m and shown that this mechanism is feasible with evidence from molecular modeling. Briefly, we have argued that:

1. A helix-coil transition in a key region of the chain (following residues 167/168) perfectly disposes this region to loop around and bind to the empty peptide-binding cleft of the molecule, in an act of auto-display.
2. What potentially facilitates such a conformational transformation and binding of a section of the B27 chain by its own peptide-binding cleft is: (a) the proximity of residue 168 to the N-terminus of any normally bound peptide ligand, (b) the fact that the region of the chain immediately following the helix beginning with residue 168 constitutes an interdomain segment separating the α3 domain from the combined α1 and α2 domains, which may be expected to be flexible enough in a β2m-free B27 chain to cause unfolding of the helix and (c) the fact that the proposed helix-coil transition in the region actually occurs during high temperature molecular dynamics, and stably survives subsequent dynamics.
3. High-affinity binding of the region following residue 168 to the B27 peptide-binding cleft is made probable by the fact that the region contains a sequence of residues (RRYLENGKETLQR, between residues 169 and 181) that exactly matches the known sequence of a natural peptide ligand of B27 (N-RRYLENGKETLQR-C).
4. Such 'auto-display' is further made feasible by the fact that B27 retains peptide-binding capability in the absence of bound β2m, which is something that has been recently shown, as well as proposed for disulfide-bonded misfolded forms of B27. Auto-display is also made feasible by the fact that it is expected to destroy the A pocket of the peptide-binding cleft, facilitating entry of sections of the polypeptide chain constituting pocket A (e.g., residues 167 and 171) into the cleft, and occupation of the cleft by residues 169–177 of the B27 chain, with residues up until residue 179 having some peripheral associations with the cleft, and residues 180 and 181 remaining outside the cleft to facilitate rotational optimization of interactions with the α3 domain.

We would like to emphasize that whereas we have suggested a mechanism for auto-display to occur in a principally unimolecular fashion, it could also conceivably occur in bimolecular, or multimolecular fashion, with each molecule binding to a section of a neighboring molecule's chain. This would ensure that B27 could potentially exist in a structured form within large multimolecular assemblies. We have recently obtained experimental evidence (to be published separately) for the existence of such structured assemblies using peptide-free, β2m-free B27 chains.

The modeling studies show that the really important section involved in autodisplay is the stretch between residues 169 and 179 (or even 169 and 177), since residues 178 and 179 are only peripherally associated with the cleft, and residues 180 and 181 appear to be outside the cleft and in the section forming the link to the α3 domain. Therefore, upon first consideration, it might be argued that any molecule of B27 containing residues 169–177 should be capable of forming the proposed auto-displaying, or cross-displaying structure(s). Yet, all B27 subtypes are not associated with disease. Also, all subtypes do not bind with similar affinities to residues 169–177, or residues 169–179, when these residues are presented to β2m-bound B27 as free peptides. Certain details regarding these aspects of binding behavior were given in Section 2.2, and further details may be found in a recent publication [25]. What might be the reasons for such differences in behavior amongst B27 subtypes if indeed all contain residues 169–177? We feel that a number of different explanations might apply, either singly or in combinations. Firstly, there could be differences in the tendencies of the various B27 subtypes to dissociate from β2m, rather than differences in their individual abilities to bind (or not bind) residues 169–181, once the heavy chain becomes β2m-free. Secondly, there could be differences in the relative conformational stabilities of the native-like B27 conformation in the β2m-free form, which would determine whether only a helix-coil transition would occur initially, allowing the chain to quickly undergo auto-display, or whether the whole β2m-free molecule would spontaneously undergo unfolding as is thought to occur classically with MHC Class I molecules, leaving no scope for auto-display. Thirdly, there could be differences in the relative flexibilities of the various B27 forms around the region (residues 167/168) in which the chain turns around to occupy the peptide-binding cleft before descending to the α3 domain. Such differences could owe to mutation-linked differences in the environments of residues 167/168 in various subtypes. Fourthly, certain mutation-linked differences in the environments offered by the peptide-binding cleft(s) of various B27 forms could themselves modulate the affinities of such clefts for residues from the 169–169 section of the chain when it is presented as a part of the whole B27 chain. Therefore, the presence of residues 169–179 would not automatically entitle an MHC Class I chain of the B27 variety to undergo auto-display; other factors as listed above could also play a role in determining whether auto-display would occur.

Another issue that bears reiteration is the question of whether the conformationally rearranged B27 would be presented to TCRs. We have already discussed this in some detail in the latter half of Section 2.3, and argued that from a purely physical, or steric, point of view, TCRs would be able to access autodisplaying B27. Of course, this does not address the question of whether TCRs capable of recognizing the auto-displaying B27 molecules would be available in the system. We have argued that they are likely to be available, since the appearance of β2m-free B27 heavy chains occurs after the developmental stage at which most thymic education of T-cells occurs. However, it is possible that all T-cell clones conceivable may not be available, or that only certain varieties of TCRs might engage in binding to β2m-free B27. For instance, for disulfide-bonded homodimers of misfolded B27 it has been suggested that peptides displayed and bound by these forms may be recognized by γ/δ chain TCRs rather than by α/β chain TCRs [26]. The same could apply here. We have no specific comments to make regarding this, at this time, other than to say that T-cell responses of both helper and effector types could occur.

Disulfides could aid the formation and survival of molecules assembled through cross-display. Indeed, structural analysis suggests that it is conceivable for residues such as Cys67 and Cys164, which are known to be involved in B27 associations [11,14,27], to be brought together by cross-chain auto-display involving neighboring molecules. Cys164 is a residue that is proximal to residues 168/169 in the chain and so it would automatically be positioned near the region of the cleft adjacent to the N-terminus of any ordinarily bound peptide. Likewise, Cys67 is proximal to Arg62 which locks in the N-terminus of any ordinarily bound peptide in various MHC class I molecules [28]. Thus, with some minor structural readjustments, residues 67 and 164 of neighboring chains (carrying out cross-chain auto-display, or cross-display, of the kind proposed here) could easily be conceived to form interchain disulfide bonds, in addition to the Cys67–Cys67, and Cys164–Cys164, disulfide bonds already proposed for misfolded homodimers. It may be remarked here that it is mainly Cys67 that has been implicated in homodimer formation through disulfide bonding at the cell surface [14]. The involvement of Cys164 has so far been implicated only for homodimers formed in the ER that, interestingly, are thought to retain much of the native conformation of the heavy chain [27]. Interestingly, one form of homodimer formed in the ER (which reacts with the W6/32 mAb antibody) has been stated to be likely to reach the cell surface from the ER [11], suggesting that the cell surface might indeed end up displaying homodimers formed through disulfide bonds involving Cys67 as well as Cys164. The form(s) involving Cys67 disulfide bonding would be anticipated to result from in situ misfolding of B27 on the cell surface following shedding of β2m. The form(s) involving Cys164, on the other hand, would be anticipated to result from transport of misfolded B27 from the ER to the cell surface. Our interest is in pointing out how cross-display of residues 169–181 between neighboring molecules appears to be compatible with the formation of disulfide bonds involving Cys67 and/or Cys164. It is possible that the interchain disulfides observed to form in β2m-free B27 chains actually form because B27 chains bind and display each other's polypeptide segments within their peptide-binding clefts, and that this happens sometimes in an interaction involving only two molecules (shutting off further scope for extended cross-display) and sometimes in interactions involving many more molecules, because once the process starts with one molecule binding the next molecule's chain and the next molecule binding the chain of the molecule lying next to it, and so on, the process may not end until steric reasons owing to physical curving of such assemblies force the assembly to stop. This reconciles our proposal with hypothesis B mentioned in the introduction, since experimental evidence for that hypothesis, in fact, indicates that misfolded B27 chains can form either homodimers, or large assemblies of chains, but no other species of intermediate size. In addition, our proposal also reconciles hypotheses A and D with hypothesis B, because (i) we invoke and use the concept of the arthritogenic self peptide (except that we propose that the relevant residue sequence that is bound and displayed is actually a part of the intact B27 chain), and (ii) we propose the formation of a profoundly conformationally altered B27 that is argued to be likely to stimulate all arms of the immune system, including the B-cell system that could produce antibodies against a foreign (misfolded) conformation of a naturally occuring (self) protein.

We suggest that the following types of experiments could be done to test the hypothesis and are currently engaged in carrying out some of these experiments. Firstly, specific mutations could be made that would allow B27 to fold and bind other peptides in the classical fashion, but lose the ability to bind to peptides equivalent to residues 169–181 (or a shorter form, like 169–179) due to alterations in pocket environments within clefts. Such forms could be tested for their ability to adopt structured, misfolded assemblies vis a vis their tendency to unfold in the absence of β2m like ordinary class I MHCs, to examine which mode of behavior would be adopted. Secondly, limited mutations in the 169–179 region could be made to convert the B27 MHCs into other MHCs of the B variety, followed up with monitoring of conformational behavior in the absence of β2m. Thirdly, chemical cross-linking experiments combined with proteolysis carried out with a protease of known specificity could be done to examine whether any masses corresponding to cross-links likely to be formed by auto-display are observed. Fourthly, dissociation parameters (energies, etc.) of soluble assemblies of β2m-free B27 could be determined under mildly destabilizing conditions, together with monitoring of conformational changes, to examine whether the observed behavior is compatible with the dissociation of residues from peptide-binding clefts. Finally, protein assemblies could be proteolyzed with, or without, reduction of disulfide bonds, to see whether the resulting forms could be crystallized and studied to reveal hints of any auto- or cross-display.

Acknowledgements: M.L.-G. thanks the Department of Biotechnology, Government of India, for funding to study the link between HLA misfolding and disease from theoretical as well as experimental standpoints.

References

[1] Brewerton, D.A., Caffrey, M., Hart, F.D., James, D.C.O., Nichols, A. and Sturrock, R.D. (1973) Lancet 1, 904.
[2] Scofield, R.H., Kurien, B., Gross, T., Warren, W.L. and Harley, J.B. (1995) Lancet 345, 1542–1544.
[3] Benjamin, R. and Parham, P. (1992) Rheum. Dis. Clin. North Am. 18, 11–21.
[4] Ringrose, J.H., Yard, B.A., Muijsers, A., Bog, C.J. and Feltkamp, T.E. (1996) Clin. Rheumatol. 15, 74–78.
[5] Lahesmaa, R., Skurnik, M. and Toivanen, P. (1993) Immunol. Res. 12, 193–208.
[6] Schwimmbeck, P.L., Yu, D.T. and Oldstone, M.B. (1987) J. Exp. Med. 166, 173–181.
[7] Garcia, F., Marina, A., Albar, J.P. and Lopez de Castro, J.A. (1997) Tissue Antigens 49, 23–28.
[8] Alvarez, I., Sesma, L., Marcilla, M., Ramos, M., Marti, M., Camafeita, E. and de Castro, J.A.L. (2001) J. Biol. Chem. 276, 32729–32737.
[9] Malik, P., Klimovitsky, P., Deng, L.W., Boyson, J.E. and Strominger, J.L. (2002) J. Immunol. 169, 4379–4387.
[10] Allen, R.L., O'Callaghan, C.A., McMichael, A.J. and Bowness, P. (1999) J. Immunol. 162, 5045–5048.
[11] Dangoria, N.S., Delay, M.L., Kingsbury, D.J., Mear, J.P., Uchanska-Ziegler, B., Ziegler, A. and Colbert, R.A. (2002) J. Biol. Chem. 277, 23459–23468.
[12] Harris, M.R., Lybarger, L., Myers, N.B., Hilbert, C., Solheim, J.C., Hansen, T.H. and Yu, Y.Y. (2001) Int. Immunol. 13, 1275–1282.
[13] Xie, J., Wang, Y., Freeman, M.E., Barlogie, B. and Yi, Q. (2003) Blood 101, 4005–4012.
[14] Antoniou, A.N., Ford, S., Taurog, J.D., Butcher, G.W. and Powis, S.J. (2004) J. Biol. Chem. 279, 8895–8902.

[15] UchanskaZiegler, B. and Ziegler, A. (2003) Trends Immunol. 24, 73–76.
[16] Yong, Z., Zhang, J.J., Schaack, T., Chen, S., Nakayama, A. and Yu, D.T. (1989) Clin. Exp. Rheumatol. 7, 513–519.
[17] Boisgerault, F., Tieng, V., Stolzenberg, M-C., Dulphy, N., Khalil, I., Tamouza, R., Charron, D. and Toubert, A. (1996) J. Clin. Invest. 98, 2764–2770.
[18] Jardetzky, T.S., Lane, W.S., Robinson, R.A., Madden, D.R. and Wiley, D.C. (1991) Nature 353, 326–329.
[19] Rotzschke, O. and Falk, K. (1991) Immunol. Today 12, 447–455.
[20] Villadangos, J.A., Galocha, B., Lopez, D., Calvo, V. and de Castro, J.A.L. (1992) J. Immunol. 149, 505–510.
[21] Revillard, J.P., Vincent, C., Clot, J. and Sany, J. (1982) Eur. J. Rheumatol. Inflamm. 5, 398–405.
[22] Walters, M.T., Stevenson, F.K., Goswami, R., Smith, J.L. and Cawley, M.I. (1989) Ann. Rheumtol. Dis. 48, 905–911.
[23] Boyle, L.H. and Hill Gaston, J.S. (2003) Rheumatology 42, 404–412.
[24] Guptasarma, P. (1999) Curr. Sci. 77, 508–514.
[25] de Castro, J.A.L., Alvarez, I., Marcilla, M., Paradela, A., Ramos, M., Sesma, L. and Vasquez, M. (2004) Tissue Antigens 63, 424–445.
[26] Bowness, P., Zaccai, N., Bird, L. and Jones, E.Y. (1999) Expert Rev. Mol. Med. 26 (October), 1–10.
[27] Bird, L.A., Peh, C.A., Kollnberger, S., Elliott, T,, McMichael, A.J. and Bowness, P. (2003) Eur. J. Immunol. 33, 748–759.
[28] Hillig, R.C., Hulsmeyer, M., Saenger, W., Welfle, K., Misselwitz, R., Welfle, H., Kozerski, C., Volz, A., Uchanska-Ziegler, B. and Ziegler, A. (2004) J. Biol. Chem. 279, 652–663.